

A Pyrene-Based, Fluorescent Three-Dimensional Covalent Organic Framework

Guiqing Lin,[†] Huimin Ding,[†] Daqiang Yuan,[‡] Baoshan Wang,^{*,†} and Cheng Wang^{*,†}

[†]Key Laboratory of Biomedical Polymers (Ministry of Education), College of Chemistry and Molecular Sciences, Wuhan University, Wuhan 430072, China

[‡]State Key Laboratory of Structural Chemistry, Fujian Institute of Research on the Structure of Matter, Chinese Academy of Sciences, Fuzhou 350002, China

S Supporting Information

ABSTRACT: The targeted synthesis of 3D COFs has been considered challenging, especially adopting new topologies and bearing photoelectric units. Herein, for the first time, we report the synthesis and characterization of a novel 3D pyrene-based COF (3D-Py-COF), by selectively choosing the geometry of the precursors and the connection patterns. Based on X-ray diffraction measurement and detailed simulations, 3D-Py-COF is proposed to adopt a two-fold interpenetrated **pts** topology, which has never been reported before. In addition, 3D-Py-COF has a narrow pore size distribution and high surface area and also features selective absorption of CO₂ over N₂. Interestingly, due to the existence of isolated pyrene units in the 3D framework, 3D-Py-COF is the first fluorescent 3D COF and can be used in explosive detection. Our results not only show it is possible to rationally design and synthesize 3D COFs with other topologies but also demonstrate that the incorporation of photoelectric units into 3D COFs can allow the resulting materials with interesting properties.

Covalent organic frameworks (COFs) represent an emerging class of crystalline polymers with structural periodicity and inherent porosity.^{1–3} Due to their high surface area, low density, and high thermal stability, COFs have attracted considerable attention over the past decade as promising applications in gas storage^{4–8} and catalysis.^{9–13} Depending on the connectivity and geometry of the selected molecular building blocks, COFs can be categorized into either two-dimensional (2D) layered structures or three-dimensional (3D) networks. For the former, the most important feature is that the 2D flat sheets stack in a face-to-face mode with maximal π -orbital overlap, which can facilitate the charge migration through the framework. Therefore, with certain photoelectric moieties embedded into the well-defined 2D COFs, the resulting 2D COFs materials can possess unique optical or electrical properties.¹⁴ Various photoelectric units, such as pyrene,^{15–17} porphyrin,^{18–21} phthalocyanine,^{22–24} thiophene,^{25–27} and tetrathiafulvalene,^{28–30} have been successfully developed for 2D COFs, and the resulting materials have found interesting application in optoelectronic device. Thanks to the effort of many groups, the design and synthesis of 2D COFs have been relatively well established.^{31–36}

Unlike the layered structures of 2D COFs, the molecular building blocks in 3D COFs are three-dimensionally organized to form the extended network. As a result, 3D COFs can characteristically possess high specific surface area, low densities, and, more importantly, numerous open sites. Like 3D metal–organic frameworks, 3D COFs may also have potential applications in many different fields, such as gas storage,^{37–41} catalysis,⁴² biology,⁴³ etc. However, since Yaghi et al. reported the first 3D COF in 2007,⁴⁴ only a few 3D COFs have been announced over the past years.^{37–46} The big challenge is how to rationally design and synthesize precursors with the right geometry and connection patterns and then construct 3D COFs with the desirable topology. Until now, due to the limitation of available molecular building blocks, all the reported 3D COFs adopt a topology belonging to one of three nets (**dia**,^{37,38,43,45,46} **bor**,⁴⁴ or **ctn**^{39–42,44}). As such, the rational design and synthesis of 3D COFs with other topologies are highly desirable. Moreover, the incorporation of photoelectric units into 3D COFs, which can allow the photoelectric units isolated in the 3D framework and the resulting materials with interesting properties, has seldom been reported. Therefore, the targeted synthesis of 3D COFs bearing photoelectric units is also highly demanded.

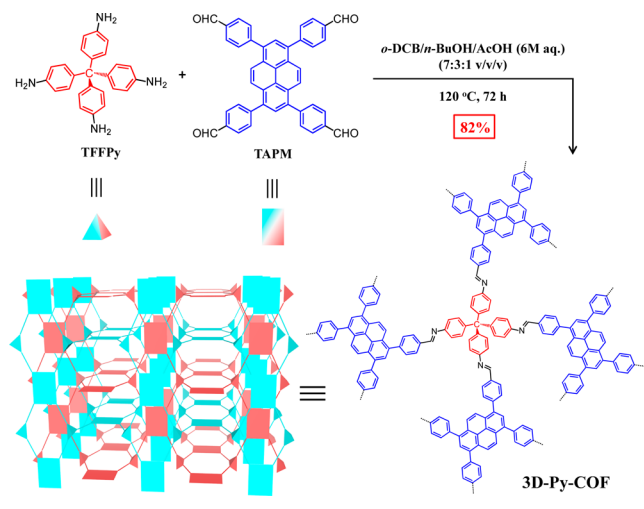
Herein, by selectively choosing the geometry of the precursors and the connection patterns, we demonstrate for the first time the synthesis and characterization of a novel 3D pyrene-based COF, namely 3D-Py-COF (Scheme 1). Based on X-ray diffraction measurement and detailed simulations, we can conclude 3D-Py-COF adopts a two-fold interpenetrated **pts** topology, which has never been reported before. In addition, the gas absorption experiments indicate that 3D-Py-COF has a narrow pore size distribution and high surface area and also features selective absorption of CO₂ over N₂. Interestingly, due to the existence of isolated pyrene units in the 3D framework, 3D-Py-COF is the first fluorescent 3D COF and can be used in explosive detection.

In order to synthesize 3D-Py-COF, we propose utilizing tetrahedral (3D-*T_d*) and rectangle (2D-*C₂*) building blocks, which can be further connected through [4 + 4] imine condensation reactions. Therefore, we chose the reported tetra(*p*-aminophenyl)methane (TAPM)³⁷ with four amine groups and 1,3,6,8-tetrakis(4-formylphenyl) pyrene

Received: January 19, 2016

Published: February 29, 2016

Scheme 1. Schematic Representation of the Synthesis and Extended Two-Fold Interpenetrated Structure of 3D-Py-COF



(TFFPy)¹⁵ with four aldehyde groups as the precursors. By condensing TAPM and TFFPy in the mixture of *o*-dichlorobenzene/*n*-butanol/acetic acid (7:3:1, by vol.) at 120 °C for 72 h (Scheme 1), 3D-Py-COF was isolated as a yellow powder that was insoluble in common organic solvents. The formation of imine linkages in 3D-Py-COF was confirmed by Fourier transform infrared (FT-IR) and ¹³C cross-polarization with total suppression of sidebands (CP-TOSS) NMR spectroscopic methods. The FT-IR spectrum of 3D-Py-COF clearly revealed the C=N stretching modes characteristic for imines at 1626 cm⁻¹ (Figure S1), whereas the ¹³C CP-TOSS NMR spectrum (Figure S2) showed a resonance at 156 ppm for carbon of C=N bond. In addition, thermogravimetric analysis showed that 3D-Py-COF has high thermal stability up to 550 °C (Figure S3), and scanning electron microscopy revealed that 3D-Py-COF has a granular morphology (Figure S4).

A powder X-ray diffraction (PXRD) experiment was performed to assess the crystallinity and unit cell parameters of 3D-Py-COF. As shown in Figure 1 (black curve), 3D-Py-

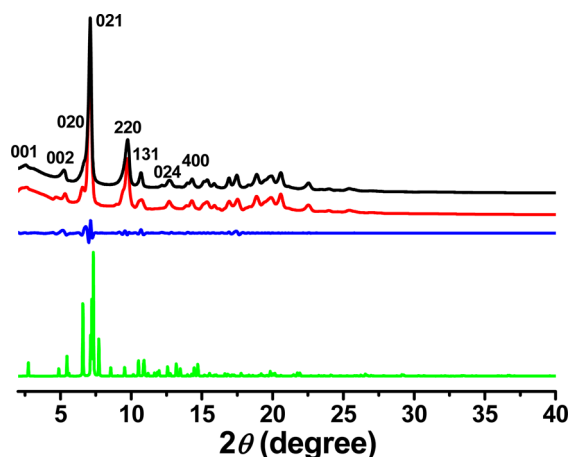


Figure 1. PXRD patterns of 3D-Py-COF. PXRD profiles of experimental pattern (black curve), Pawley refined (red curve), and calculated (green curve) patterns from the two-fold interpenetrated pts modeled structure; their difference (blue curve).

COF exhibited amounts of intense diffraction peaks, indicating its crystalline nature. To elucidate the lattice packing, we constructed the crystal model using Materials Studio software package. Considering the geometry of the precursors and the connection patterns, a few nets (e.g., **pth**, **pti**, **ptt**, **pts**, etc.) for 3D-Py-COF are reasonable according to reticular chemistry structure resource (RCSR).⁴⁷ Modeling was then performed accordingly using density functional tight-binding method including Lennard-Jones dispersion (DFTB-D, see Section S4 for details). Among them, the calculated PXRD patterns (Figure 1, green curve) of the simulated structure based on two-fold interpenetrated **pts** net (Figure 2) with *Cmmm* space

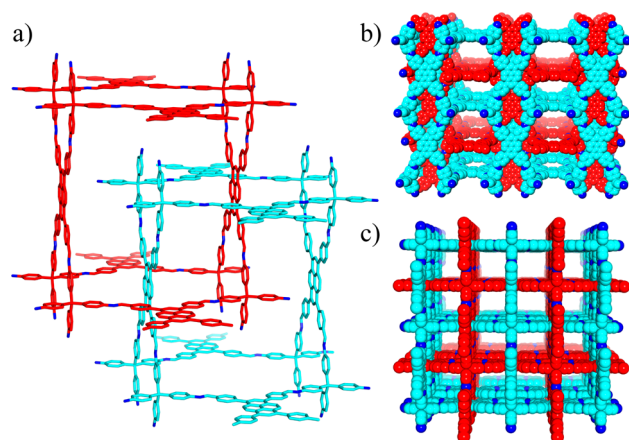


Figure 2. Structural representations of 3D-Py-COF. (a) two-fold interpenetrated **pts** network; (b) space-filling model viewed from *A* axis; (c) space-filling model viewed from *C* axis. Carbon, red or cyan; nitrogen, blue; and hydrogen atoms are omitted for clarity.

group were in agreement with the experimental ones. Furthermore, the Pawley refinement yielded an XRD pattern (Figure 1, red curve) that is in good agreement with the experimentally observed pattern, as evident by their negligible difference (Figure 1, blue curve) compared with the experimental data. The refinement results yield a unit cell with parameters of $a = 24.4130 \text{ \AA}$, $b = 26.6441 \text{ \AA}$, $c = 32.6337 \text{ \AA}$, which are very similar to those of suggested model ($a = 24.5076 \text{ \AA}$, $b = 26.8437 \text{ \AA}$, $c = 32.3974 \text{ \AA}$). The final wR_p and R_p values converged to 8.29 and 5.41%, respectively. In contrast, for other possible structures, the calculated PXRD patterns were not in agreement with the experimental ones (see SI, Section 4). For example, the calculated PXRD patterns (Figure S6) of model based on **pth** net with $P6_222$ space group showed several peaks below 7°, which were inconsistent with the experimental data. On the basis of these calculations, 3D-Py-COF is proposed to adopt a two-fold interpenetrated **pts** topology (Figure 2).

The permanent porosity of 3D-Py-COF was determined by measuring the nitrogen adsorption of freshly activated samples at 77 K. As shown in Figure 3a, 3D-Py-COF displayed type I isotherm with a sharp uptake under low relative pressures region ($P/P_0 < 0.1$), which is a characteristic of microporous materials. The Brunauer–Emmett–Teller surface area and total pore volume were calculated as 1290 m² g⁻¹ and 0.72 cm³ g⁻¹, respectively. The pore size distribution analysis based on the quenched solid density functional theory model exhibited a major peak centered at 0.59 nm and two minor ones at 0.89 and 1.05 nm (Figure 3b). Given the microporous nature and the narrow pore size distribution of 3D-Py-COF, we then

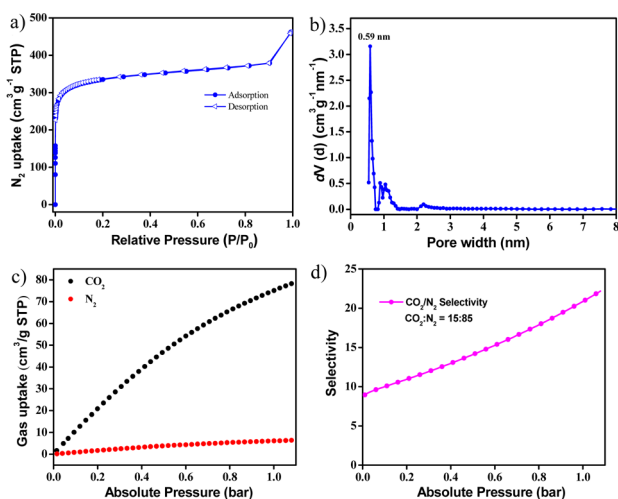


Figure 3. Gas sorption measurements for 3D-Py-COF. (a) N_2 sorption isotherm at 77 K. (b) Pore size distribution from the quenched solid density functional theory. (c) CO_2 and N_2 isotherms at 273 K. (d) IAST selectivity of CO_2/N_2 at the ratio of 15/85.

investigated its gas uptake capacities of CO_2 and N_2 at 273 K. As shown in Figure 3c, the CO_2 isotherm exhibited a smooth rise at low pressures and reached a value of $78.2 \text{ cm}^3 \text{ g}^{-1}$ at 1.08 bar. In contrast, the N_2 uptake at 1.08 bar was only $6.4 \text{ cm}^3 \text{ g}^{-1}$. To predict the selectivity of CO_2 versus N_2 at 273 K, we next used the ideal adsorbed solution theory (IAST) to calculate the multicomponent adsorption behavior from the experimental pure-gas isotherms. The adsorption selectivity for CO_2/N_2 mixtures (15/85 molar ratio) of 3D-Py-COF as a function of pressure was presented in Figure 3d. The selectivity of CO_2 over N_2 showed a smooth increase between 0 and 1.08 bar and reached 22.2 at 1.08 bar. The calculated isosteric heat of adsorption (Q_{st}) at zero-coverage for CO_2 using the virial method was $\sim 17.4 \text{ kJ mol}^{-1}$.

Very interesting, 3D-Py-COF showed an intense yellow-green luminescence (Figure 4a). To our best knowledge, this is

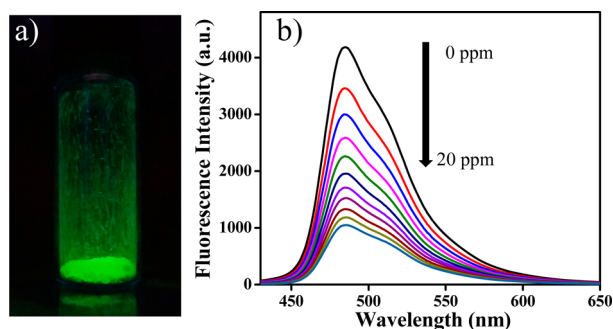


Figure 4. Fluorescent behavior of 3D-Py-COF. (a) Photograph of the 3D-Py-COF powders under UV light irradiation. (b) Fluorescence quenching upon addition of PA (0–20 ppm) in DMF ($\lambda_{ex} = 408 \text{ nm}$).

the first fluorescent 3D COF. Upon excitation at 408 nm, the suspension of 3D-Py-COF in DMF emitted a band centered at 484 nm. This phenomenon is totally different from that of the reported imine-linked 2D Py-COFs (ILCOF-1,¹⁵ Py-DHPh COF,¹⁶ etc.), which are nonfluorescent. We believe the fluorescence of 3D-Py-COF most likely originated from the isolated imine-functionalized pyrene units in the 3D network, which can be further supported by the fluorescence study of

model compound (Scheme S1 and Figure S14). Since 3D-Py-COF is porous and fluorescent, we then investigated its chemosensing behavior by choosing the commercially available picric acid (PA) as the explosive model. Figure 4b showed the fluorescence spectra of 3D-Py-COF with addition of different amounts of PA. Obviously, the fluorescence of 3D-Py-COF was quenched when PA was gradually added into the suspension. The fluorescence quenching degrees reaches to 75% when the concentration of PA is 20 ppm, indicating 3D-Py-COF is sensitive to PA. The Stern–Volmer curve quenching constant (K_{sv}) is estimated to be $3.1 \times 10^4 \text{ M}^{-1}$.

In summary, we have reported for the first time the design and synthesis of a novel 3D pyrene-based COF, starting from tetrahedral and rectangle building blocks that are connected through [4 + 4] imine condensation reactions. The detailed simulations suggest that 3D-Py-COF is proposed to adopt two-fold interpenetrated pts topology, which has never been reported before. In addition, 3D-Py-COF shows high thermal stability and surface area and also features selective absorption of CO_2 over N_2 . Interestingly, due to the existence of isolated pyrene units in the 3D framework, 3D-Py-COF is the first fluorescent 3D COF with a yellow-green luminescence and has shown potential application in explosive detection. Based on these results, we can conclude that it is possible to rationally design and synthesize 3D COFs with other topologies, and we believe more 3D COFs can be expected. Moreover, as the building blocks are isolated in the 3D network, the incorporation of photoelectric units into 3D COF can result in materials with interesting properties that may be different than that of 2D analogues. Considering their interesting properties and promising applications, the design and synthesis of 3D COFs with other topologies and bearing other photoelectric units are undergoing in our lab.

■ ASSOCIATED CONTENT

📄 Supporting Information

The Supporting Information is available free of charge on the ACS Publications website at DOI: 10.1021/jacs.6b00652.

Experimental details and data (PDF)

■ AUTHOR INFORMATION

✉ Corresponding Author

*chengwang@whu.edu.cn

Notes

The authors declare no competing financial interest.

■ ACKNOWLEDGMENTS

This work was supported by National Natural Science Foundation of China (21572170, 21273166), the Research Fund for the Doctoral Program of Higher Education of China (20130141110008), the Outstanding Youth Foundation of Hubei Province (2015CFA045), the Beijing National Laboratory for Molecular Sciences, and the Open Foundation of State Key Laboratory of Electronic Thin Films and Integrated Devices (KFJJ201505). We thank Prof. Zhongming Sun (from Changchun Institute of Applied Chemistry, Chinese of Academy of Sciences) for kind discussions.

■ REFERENCES

- (1) Waller, P. J.; Gándara, F.; Yaghi, O. M. *Acc. Chem. Res.* **2015**, *48*, 3053.
- (2) Ding, S. Y.; Wang, W. *Chem. Soc. Rev.* **2013**, *42*, 548.

- (3) Feng, X.; Ding, X.; Jiang, D. *Chem. Soc. Rev.* **2012**, *41*, 6010.
- (4) Huang, N.; Chen, X.; Krishna, R.; Jiang, D. *Angew. Chem., Int. Ed.* **2015**, *54*, 2986.
- (5) Yang, H.; Du, Y.; Wan, S.; Trahan, G. D.; Jin, Y.; Zhang, W. *Chem. Sci.* **2015**, *6*, 4049.
- (6) Zhou, T. Y.; Xu, S. Q.; Wen, Q.; Pang, Z. F.; Zhao, X. *J. Am. Chem. Soc.* **2014**, *136*, 15885.
- (7) Song, J. R.; Sun, J.; Liu, J.; Huang, Z. T.; Zheng, Q. Y. *Chem. Commun.* **2014**, *50*, 788.
- (8) Doonan, C. J.; Tranchemontagne, D. J.; Glover, T. G.; Hunt, J. R.; Yaghi, O. M. *Nat. Chem.* **2010**, *2*, 235.
- (9) Lin, S.; Diercks, C. S.; Zhang, Y. B.; Kornienko, N.; Nichols, E. M.; Zhao, Y.; Paris, A. R.; Kim, D.; Yang, P.; Yaghi, O. M.; Chang, C. J. *Science* **2015**, *349*, 1208.
- (10) Xu, H.; Gao, J.; Jiang, D. *Nat. Chem.* **2015**, *7*, 905.
- (11) Vyas, V. S.; Haase, F.; Stegbauer, L.; Savasci, G.; Podjaski, F.; Ochsenfeld, C.; Lotsch, B. V. *Nat. Commun.* **2015**, *6*, 8508.
- (12) Shinde, D. B.; Kandambeth, S.; Pachfule, P.; Kumar, R. R.; Banerjee, R. *Chem. Commun.* **2015**, *51*, 310.
- (13) Ding, S. Y.; Gao, J.; Wang, Q.; Zhang, Y.; Song, W. G.; Su, C. Y.; Wang, W. *J. Am. Chem. Soc.* **2011**, *133*, 19816.
- (14) Dogru, M.; Bein, T. *Chem. Commun.* **2014**, *50*, 5531.
- (15) Rabbani, M. G.; Sekizkardes, A. K.; Kahveci, Z.; Reich, T. E.; Ding, R.; El-Kaderi, H. M. *Chem. - Eur. J.* **2013**, *19*, 3324.
- (16) Chen, X.; Huang, N.; Gao, J.; Xu, H.; Xu, F.; Jiang, D. *Chem. Commun.* **2014**, *50*, 6161.
- (17) Dalapati, S.; Jin, S.; Gao, J.; Xu, Y.; Nagai, A.; Jiang, D. *J. Am. Chem. Soc.* **2013**, *135*, 17310.
- (18) Chen, X.; Addicoat, M.; Jin, E.; Zhai, L.; Xu, H.; Huang, N.; Guo, Z.; Liu, L.; Irle, S.; Jiang, D. *J. Am. Chem. Soc.* **2015**, *137*, 3241.
- (19) Calik, M.; Auras, F.; Salonen, L. M.; Bader, K.; Grill, I.; Handloser, M.; Medina, D. D.; Dogru, M.; Löbermann, F.; Trauner, D.; Hartschuh, A.; Bein, T. *J. Am. Chem. Soc.* **2014**, *136*, 17802.
- (20) Kandambeth, S.; Shinde, D. B.; Panda, M. K.; Lukose, B.; Heine, T.; Banerjee, R. *Angew. Chem., Int. Ed.* **2013**, *52*, 13052.
- (21) Wan, S.; Gándara, F.; Asano, A.; Furukawa, H.; Saeki, A.; Dey, S. K.; Liao, L.; Ambrogio, M. W.; Botros, Y. Y.; Duan, X.; Seki, S.; Stoddart, J. F.; Yaghi, O. M. *Chem. Mater.* **2011**, *23*, 4094.
- (22) Spittler, E. L.; Dichtel, W. R. *Nat. Chem.* **2010**, *2*, 672.
- (23) Spittler, E. L.; Colson, J. W.; Uribe-Romo, F. J.; Woll, A. R.; Giovino, M. R.; Saldivar, A.; Dichtel, W. R. *Angew. Chem., Int. Ed.* **2012**, *51*, 2623.
- (24) Jin, S.; Ding, X.; Feng, X.; Supur, M.; Furukawa, K.; Takahashi, S.; Addicoat, M.; El-Khouly, M. E.; Nakamura, T.; Irle, S.; Fukuzumi, S.; Nagai, A.; Jiang, D. *Angew. Chem., Int. Ed.* **2013**, *52*, 2017.
- (25) Bertrand, G. H.; Michaelis, V. K.; Ong, T. C.; Griffin, R. G.; Dincă, M. *Proc. Natl. Acad. Sci. U. S. A.* **2013**, *110*, 4923.
- (26) Dogru, M.; Handloser, M.; Auras, F.; Kunz, T.; Medina, D.; Hartschuh, A.; Knochel, P.; Bein, T. *Angew. Chem., Int. Ed.* **2013**, *52*, 2920.
- (27) Feldblyum, J. I.; McCreery, C. H.; Andrews, S. C.; Kurosawa, T.; Santos, E. J.; Duong, V.; Fang, L.; Ayzner, A. L.; Bao, Z. *Chem. Commun.* **2015**, *51*, 13894.
- (28) Ding, H.; Li, Y.; Hu, H.; Sun, Y.; Wang, J.; Wang, C.; Wang, C.; Zhang, G.; Wang, B.; Xu, W.; Zhang, D. *Chem. - Eur. J.* **2014**, *20*, 14614.
- (29) Jin, S.; Sakurai, T.; Kowalczyk, T.; Dalapati, S.; Xu, F.; Wei, H.; Chen, X.; Gao, J.; Seki, S.; Irle, S.; Jiang, D. *Chem. - Eur. J.* **2014**, *20*, 14608.
- (30) Cai, S. L.; Zhang, Y. B.; Pun, A. B.; He, B.; Yang, J. H.; Toma, F. M.; Sharp, I. D.; Yaghi, O. M.; Fan, J.; Zheng, S. R.; Zhang, W. G.; Liu, Y. *Chem. Sci.* **2014**, *5*, 4693.
- (31) Zeng, Y.; Zou, R.; Luo, Z.; Zhang, H.; Yao, X.; Ma, X.; Zou, R.; Zhao, Y. *J. Am. Chem. Soc.* **2015**, *137*, 1020.
- (32) Duhović, S.; Dincă, M. *Chem. Mater.* **2015**, *27*, 5487.
- (33) Kandambeth, S.; Venkatesh, V.; Shinde, D. B.; Kumari, S.; Halder, A.; Verma, S.; Banerjee, R. *Nat. Commun.* **2015**, *6*, 6786.
- (34) Xie, Y.-F.; Ding, S.-Y.; Liu, J.-M.; Wang, W.; Zheng, Q.-Y. *J. Mater. Chem. C* **2015**, *3*, 10066.
- (35) Fang, Q.; Zhuang, Z.; Gu, S.; Kaspar, R. B.; Zheng, J.; Wang, J.; Qiu, S.; Yan, Y. *Nat. Commun.* **2014**, *5*, 4503.
- (36) Guo, J.; Xu, Y.; Jin, S.; Chen, L.; Kaji, T.; Honsho, Y.; Addicoat, M. A.; Kim, J.; Saeki, A.; Ihee, H.; Seki, S.; Irle, S.; Hiramoto, M.; Gao, J.; Jiang, D. *Nat. Commun.* **2013**, *4*, 2736.
- (37) Zhang, Y. B.; Su, J.; Furukawa, H.; Yun, Y.; Gándara, F.; Duong, A.; Zou, X.; Yaghi, O. M. *J. Am. Chem. Soc.* **2013**, *135*, 16336.
- (38) Uribe-Romo, F. J.; Hunt, J. R.; Furukawa, H.; Klöck, C.; O'Keeffe, M.; Yaghi, O. M. *J. Am. Chem. Soc.* **2009**, *131*, 4570.
- (39) Hunt, J. R.; Doonan, C. J.; LeVangie, J. D.; Côté, A. P.; Yaghi, O. M. *J. Am. Chem. Soc.* **2008**, *130*, 11872.
- (40) Bunck, D. N.; Dichtel, W. R. *Angew. Chem., Int. Ed.* **2012**, *51*, 1885.
- (41) Bunck, D. N.; Dichtel, W. R. *Chem. Commun.* **2013**, *49*, 2457.
- (42) Fang, Q.; Gu, S.; Zheng, J.; Zhuang, Z.; Qiu, S.; Yan, Y. *Angew. Chem., Int. Ed.* **2014**, *53*, 2878.
- (43) Fang, Q.; Wang, J.; Gu, S.; Kaspar, R. B.; Zhuang, Z.; Zheng, J.; Guo, H.; Qiu, S.; Yan, Y. *J. Am. Chem. Soc.* **2015**, *137*, 8352.
- (44) El-Kaderi, H. M.; Hunt, J. R.; Mendoza-Cortés, J. L.; Côté, A. P.; Taylor, R. E.; O'Keeffe, M.; Yaghi, O. M. *Science* **2007**, *316*, 268.
- (45) Beaudoin, D.; Maris, T.; Wuest, J. D. *Nat. Chem.* **2013**, *5*, 830.
- (46) Liu, Y.; et al. *Science* **2016**, *351*, 365.
- (47) O'Keeffe, M.; Peskov, M. A.; Ramsden, S. J.; Yaghi, O. M. *Acc. Chem. Res.* **2008**, *41*, 1782.